Electronic Supplementary Material (ESI) for Journal of Materials Chemistry A

Supporting Information

Characterizations of in situ grown ceria nanoparticles on reduced graphene oxide as catalyst for electro oxidation of hydrazine

Manish Srivastava[a], Ashok Kumar Das[a], Partha Khanra[a], Md. Elias Uddin[a], Nam Hoon Kim[a], Joong Hee Lee[a,b*]

[a]WCU Program, Department of BIN Fusion Technology, Chonbuk National University, Jeonju, Jeonbuk 561-756, Republic of Korea

[b]BIN Fusion Research Team, Department of Polymer & Nano Engineering, Chonbuk National University, Jeonju, Jeonbuk 561-756, Republic of Korea,

[*]Correspondence to Joong Hee Lee Fax: +82 63 270 2341; Tel: +82 63 270 2342; E-mail:jhl@jbnu.ac.kr

Raman Spectra:

As shown in Fig. S-1, Raman spectra of GO, RGO and CeO2/RGO composite were fitted by multiple Lorentzian peaks [1-2]. The calculated values of D band area (A_D) to G band area (G_A) ratio as (A_D/A_G) are summarized in Table S-1.

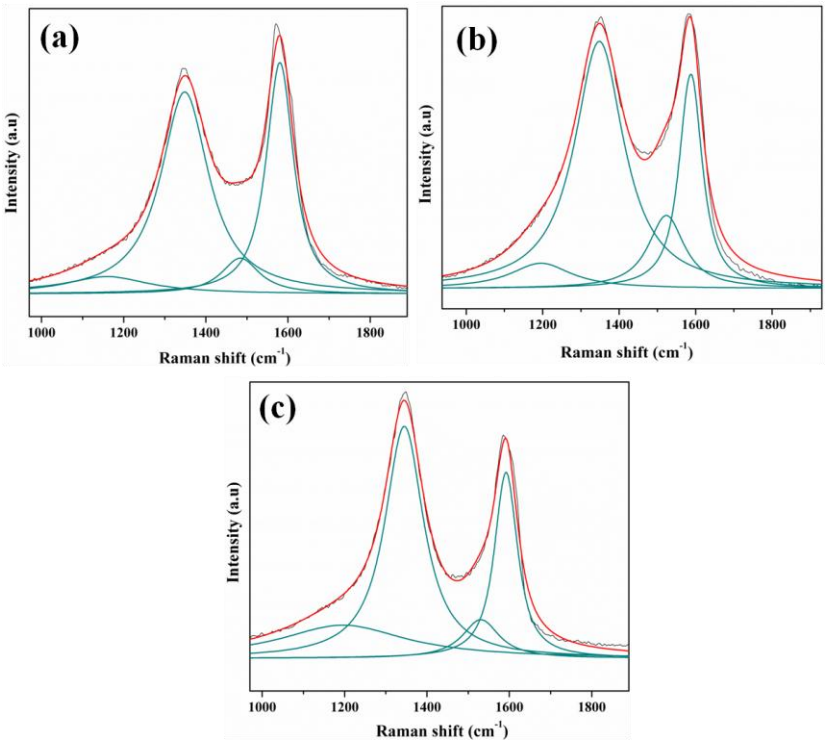

Fig. S1. Raman spectra of GO **(a)** RGO **(b)** and CeO_2/RGO composite **(c)** fitted by Lorentzian function.

Table S-1: D and G band peak area ratio calculated for GO, RGO and CeO_2/RGO samples

Sample	Peak area ratio (A_D/A_G)
GO	1.58
RGO	2.57
CeO_2/RGO	2.15

XPS analysis of Ce3d spectrum for CeO_2 and CeO_2/RGo:

The quantitative analysis for concentration of the Ce^{+3} in pure CeO_2 and CeO_2/RGo samples has been done. As shown in Fig. S2 (a, b), high resolution XPS spectra of Ce3d core were deconvoluted by mean of Gaussian-Lorentzian shape fitting using the software. The Ce 3d XPS spectra exhibit multiple states which arise from different Ce 4f level occupancies in the final state and can be labelled according to the convention established by Burroughs et al. [3], where V and U refer to the $3d_{5/2}$ and $3d_{3/2}$ spin-orbital components. The peaks labelled as U, U", U"', V, V", and V"' are corresponding to the features of Ce^{+4}, whereas; peaks referred to V' and U' are corresponding to Ce^{+3}. The concentration of Ce^{+3} was calculated by taking the ratio of the integrated peak areas corresponding to the Ce^{+3} peaks to the total area under the whole Ce 3d spectrum. Our estimate of Ce^{3+} concentration in pure CeO_2 and CeO_2/RGo samples was determined using the following equation (Eq. 1) [4]:

$$Ce^{3+} = \frac{A_{vo} + A_{v'} + A_{uo} + A_{u'}}{A_{vo} + A_{v'} + A_{uo} + A_{u'} + A_{v} + A_{v''} + A_{v'''} + A_{u} + A_{u''} + A_{v'''}} \quad (1)$$

Where *A* denotes the area of the corresponding peaks marked as the subscript in the spectrum. The calculation exposed that the concentration of Ce^{3+} in case of CeO_2/RGO samples as ~ 14.4 % which was found to higher than concentration of Ce^{3+} (~8.5 %) in case of pure CeO_2. The relatively higher concentration of Ce^{3+} suggests the higher oxygen vacancies in the CeO_2

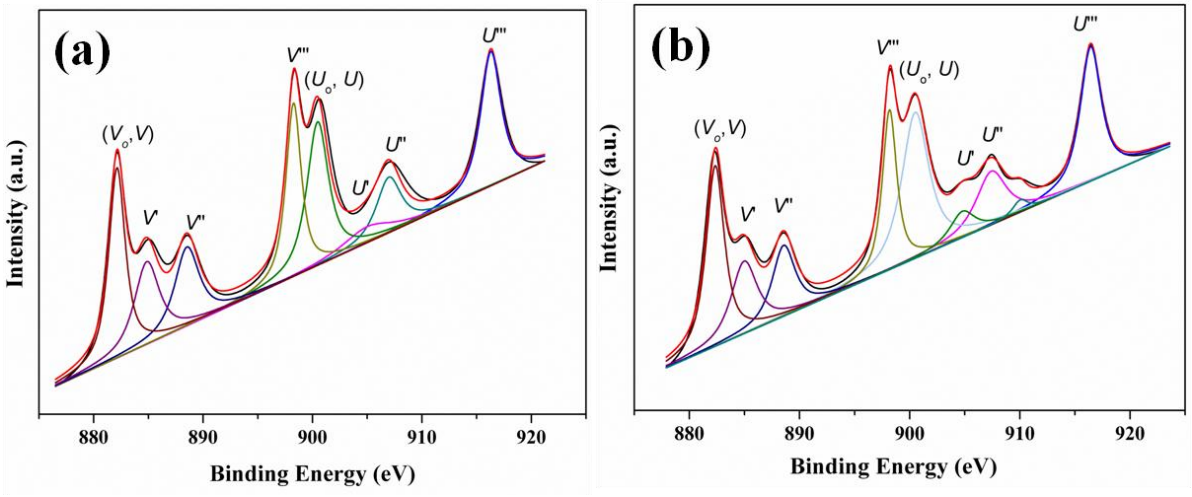

Fig. S2. XPS Ce3d spectra of CeO_2 **(a)** and CeO_2/RGO **(b)**

crystal which compensate the effective negative charge associated with the trivalent ions. Therefore, the higher concentration of Ce^{3+} in case of CeO_2/RGo may provide higher catalytic activity with compare to pure CeO_2. It was suggested that the higher concentration of Ce^{3+} (higher oxygen vacancies) may arise due to the charge transfer between the graphene and CeO_2 crystal. The above facts are also supported by the Raman analysis of the synthesized samples, where a shifting of the vibrational bands was observed in CeO_2/RGO with respect to pure CeO_2 [5].

Effect of scan rate

The effect of scan rate on electro oxidation of hydrazine was investigated and results are shown in Fig. S3 (a). It can be seen that, an increase in scan rate cause an increase in oxidation current and the peak potential shift towards the positive direction. This shift of the oxidation peak towards the more positive potential suggests an irreversible electrochemical reaction. A linear relationship between the peak current and the square root of the potential was also observed [Fig. S3 (b)], further suggest the reaction is mass transfer controlled.

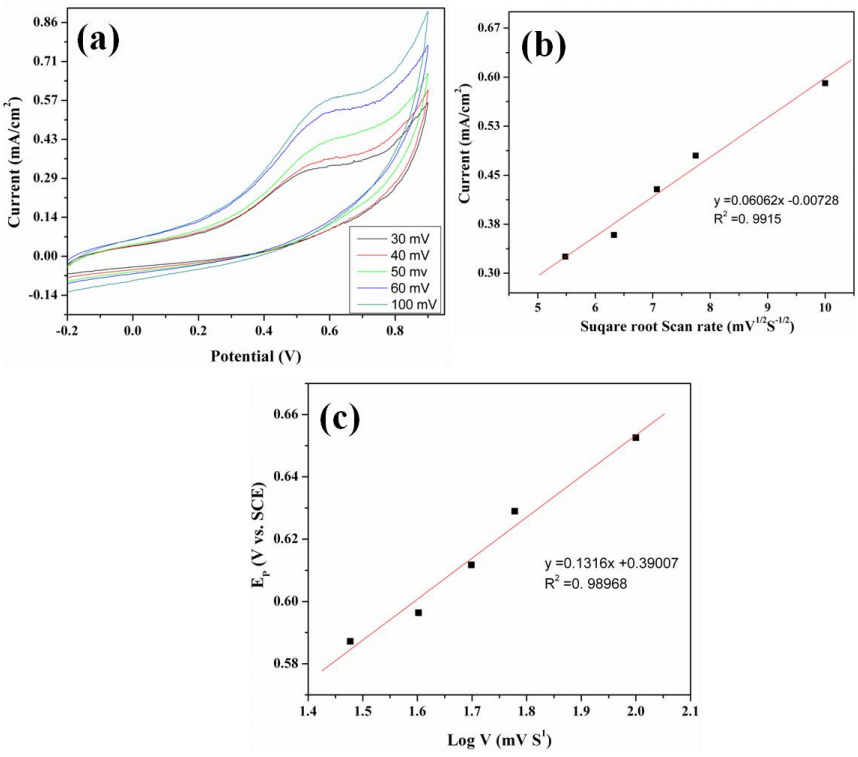

Figure S3. Cyclic voltammograms for CeO_2/RGO modified GCE in 3 M KOH containing 10 mM of hydrazine at different scan rate **(a),** plot of peak current with square root of scan rate **(b),** peak potential dependence on log v for the oxidation of hydrazine at CeO_2/RGO modified GCE **(c).**

The rate determining step was determined by Tafel slope (b) [Fig. S3 (c)], using the following equation which is valid for a totally irreversible diffusion controlled process [6].

$$E_P = \frac{b \log \nu}{2} + \text{constant} \quad (2)$$

From Eq (1), slope of E_p versus log ν plot can be given as:

$$\frac{dE_P}{d \log \nu} = \frac{b}{2} \quad (3)$$

where, ν is the scan rate and '*b*' is the Tafel slope. Additionally, the Tafel slope can also be written as:

$$b = 2.3RT(\alpha_a n_\alpha F)^{-1} \quad (4)$$

Plot of Ep vs log ν [Fig. S3 (c)], yield a slope value of 0.131, therefore *'b'*= 0.262. Assuming one electron transfer in the rate-determining step (n_α = 1), charge transfer coefficient (α) was calculated as 0.20 according to Eq. (4).

From the plot of I_p vs $\nu^{1/2}$, the number of electrons (n), involved in the overall reaction can be obtained following the Eq. (5), for totally irreversible diffusion-controlled process [7-8].

$$I_P = 3.01 \times 10^5 n[(1-\alpha)n_\alpha]^{1/2} AC_b D^{1/2} \nu^{1/2} \quad (5)$$

where, '*A*' is the electrode surface area, 'C_b' is the concentration of hydrazine and '*D*' is the diffusion coefficient. Using the D = 1.184 × 10^{-5} cm^2s^{-1}(calculated from the chronoamperometry, below), and from the slope of I_p vs $\nu^{1/2}$, the total number of electrons (n) involved in the oxidation is evaluated to be 4.

The mechanism of hydrazine significantly depends on the nature of electrode and electrolyte solution. Under the solution conditions hydrazine was mainly present in its unprotonated form and the protonated form exist in small extent. In the present study it is observed that the rate determining step is one electron transfer followed by a 3-electron process to give N_2 as the final product. The overall reaction for the electro oxidation of hydrazine in alkaline medium can be expressed as the following reaction [9-13]:

$$N_2H_4 + 4OH^- \rightarrow N_2 + 4H_2O + 4e^- \quad (I)$$

Chronoamperometric measurement

In order to get more information about the electrocatalytic process and value of diffusion coefficient, chronoamperometry measurement was conducted. Fig. S4 (a) shows the chronoampergrams obtained for various concentrations of hydrazine on the CeO_2/RGO electrode at a fixed potential of 500 mV.

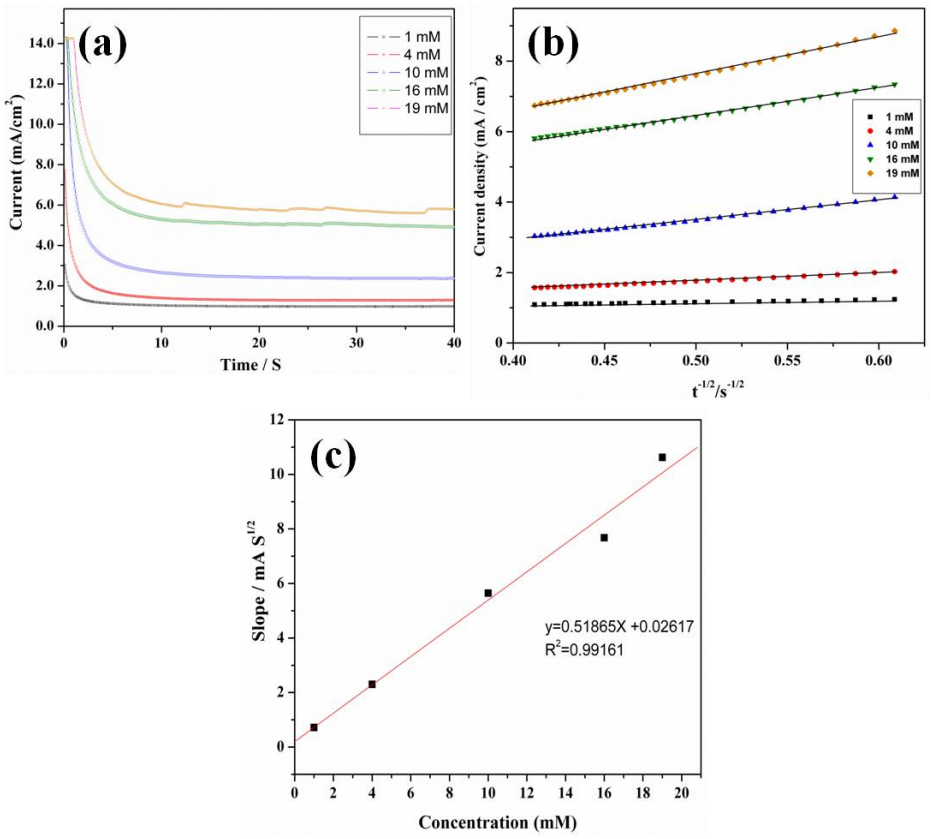

Figure S4. Chronoamperometric response of CeO_2/RGO modified GCE in 3 M KOH containing different concentration of hydrazine **(a),** plot of I vs $t^{1/2}$obtained from chronoamperometric measurement of CeO_2/RGO modified GCE at different concentration of hydrazine **(b)** relationship between the slope of the linear segment at different concentration of hydrazine **(c).**

The chronoampergrams exhibit an increase in hydrazine concentration, accompanied by an increase in anodic current. For an electroactive material, the current response under the diffusion control was described by Cottrell equation (Eq. 6):

$$I_P = nFAC_b\left(\frac{D}{\pi t}\right)^{1/2} \quad (6)$$

where, D, C_b and A are the diffusion coefficient (cm^2s^{-1}), concentration (mol cm^{-3}) and area of the electrode (cm^2), respectively. Following the Cottrell equation, the plot of *I* vs $t^{-1/2}$ as shown in Fig. S4 (b) was observed to be linear. The slope of *I* vs $t^{-1/2}$ obtained for different concentration of hydrazine was plotted in [Fig. S4 (c)] and the diffusion coefficient (D) was obtained as 1.184×10^{-5} cm^2s^{-1}. The obtained value of diffusion coefficient is agreed with earlier studies [6-8, 14].

References:

[1] A. Kaniyoor, S. Ramaprabhu, *AIP Advances*, 2012, **2,** 032183-032195.

[2] Z. Luo, C. Cong, J. Zhang, Q. Xiong, T. Yu, *Carbon*, 2012, **50,** 4252-4258.

[3] P. Burroughs, A. Hamnett, A. F. Orchard, G. Thornton, *J. Chem. Soc. Dalton Trans.* 1976, **17** 1686.

[4] M. Skoda, M. Cabala, V. Chab, K.C. Prince, L. Sedlacek, T. Skala, F. Sutara, V. Matolın, *Appl. Surf. Sci.*, 2008, **254**, 4375–4379.

[5] K. Qian, S. Lv, X. Xiao, H. Sun, J. Lu, M. Luo, W. Huang, *J Mol Catal A: Chemical* 2009, **306,** 40–47.

[6] G. K. Nezhad, R. Jafarloo, P. S. Dorraji, *Electrochim. Acta.* 2009, **54,** 5721-5726.

[7] M. Hosseini, M. M. Momeni, M. Faraji, *J Mol Catal A: Chemical*, 2011, **335**, 199-204.

[8] J. Li, H. Xie, L. Chen, *Sensor Actuat B- Chem*, 2011, **153**, 239-245.

[9] J. S. Chinchilla, K. Asazawa, T. Sakamoto, K. Yamada, H. Tanaka, P. Strasser, *J. Am. Chem. Soc.*, 2011, **133,** 5425–5431

[10] Y. Wang, Y. Wan, D. Zhang, *Electrochem commun*, 2010, **12**, 187-190.

[11] Wen Xia Yin, Zhou Peng Li, Jing Ke Zhu, Hai Ying Qin, *J. Power Sources*, 2008, **182**, 520–523.

[12] Q. Yi, W. Yu, *J. Electroanal. Chem*, 2009, **633**, 159–164.

[13] K. Yamada, K. Asazawa, K. Yasuda, T. Ioroi, H. Tanaka, Y. Miyazaki, T. Kobayashi, *J. Power Sources*, 2003, **115**, 236–242

[14] J. Zheng, Q. Sheng, L. Li, Y. Shen, *J. Electroanal. Chem*, 2007, **611**, 155-161.